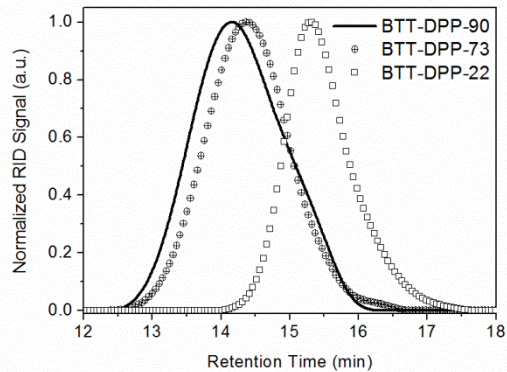


Towards Optimisation of Photocurrent from Fullerene Excitons in Organic Solar Cells

Stoichko D. Dimitrov^a, Zhenggang Huang^a, Florent Deledalle^a, Christian B. Nielsen^a, Bob C. Schroeder^a, Raja Shahid Ashraf^a, Safa Shoaei^{a,b}, Iain McCulloch^a and James R. Durrant^{*a}

5

Supporting information



10 Figure S1. GPC traces for the BTT-DPP fractions with number average molecular weights 22 (BTT-DPP-22), 73 (BTT-DPP-73) and 90 (BTT-DPP-90).

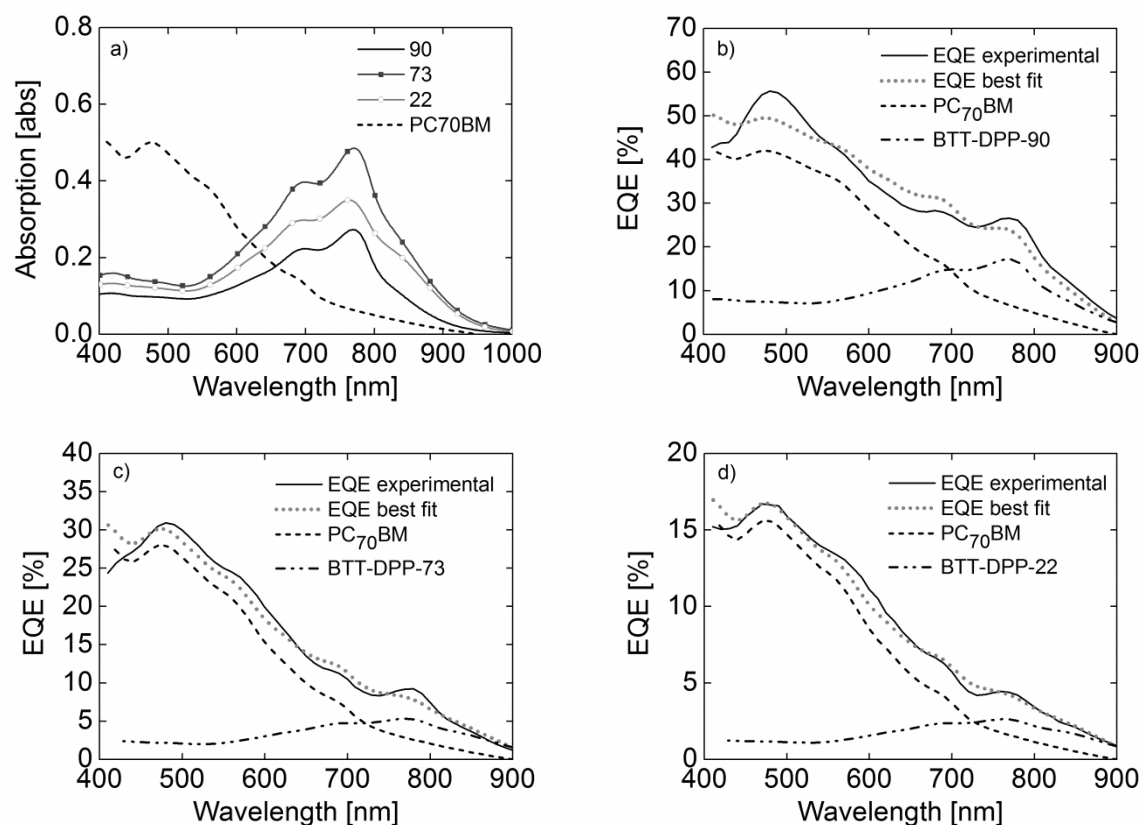


Figure S2: a) Steady-state absorption spectra of thin films of the neat BTT-DPP-90, BTT-DPP-73, BTT-DPP-22 and PC₇₀BM films. Experimentally determined EQE spectra of BTT-DPP-90/PC₇₀BM, BTT-DPP-73/PC₇₀BM and BTT-DPP-22/PC₇₀BM devices are plotted in b), c) and d), respectively. Non-linear least square fits of the EQE spectra and de-convoluted spectral contributions of PC₇₀BM and the polymers are also included in the graphs. The spectral contributions of PC₇₀BM and BTT-DPP-polymers were received by non-linear least-square fitting of their corresponding EQE spectra with the steady-state absorption spectra of the polymer and fullerene shown on Figure S2a. Error bars of the fits were 15% (b), 10% (c), 10% (d). We note that the absorption spectra used in these fits were measured on films and the corresponding fits do not take into account interference effects due to the presence of electrodes.

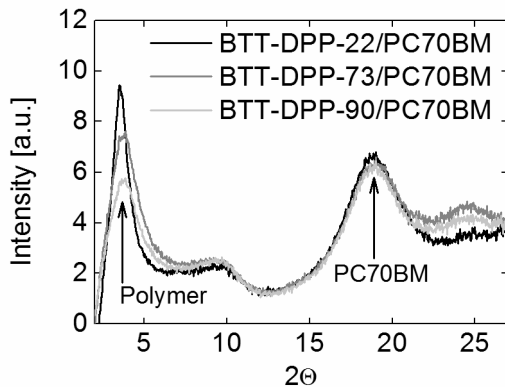


Figure S3: Wide angle X-ray scattering patterns of drop-casted films of fractionated BTT-DPP/PC₇₀BM blend films on Si/SiO₂ substrates. Polymer lamellar and PC₇₀BM stacking peaks are marked with arrows. The increase in amplitude and decrease in FWHM of these peaks show that order in the films is increasing.

M _n [kg.mol ⁻¹]	M _w [kg.mol ⁻¹]	Film thick. [nm]
90	188	100
73	155	80
22	34	50

Table S1. The table presents polymer molecular weights and thicknesses of the films as measured with a Veeco Dektak profilometer. M_w is the weight average molecular weight of the polymer. M_n is the number average molecular weight. Our previous estimates of device J_{SC} for many different systems (using the matrix-modelling technique under the assumption of 100 % IQE) as a function of thickness show that the observed here almost 4-fold increase in J_{SC} from BTT-DPP-22/PC₇₀BM to BTT-DPP-90/PC₇₀BM device (see Figure 1 and Table 1 in the main text) have origin other than changes in device thickness as confirmed by our TAS analysis.

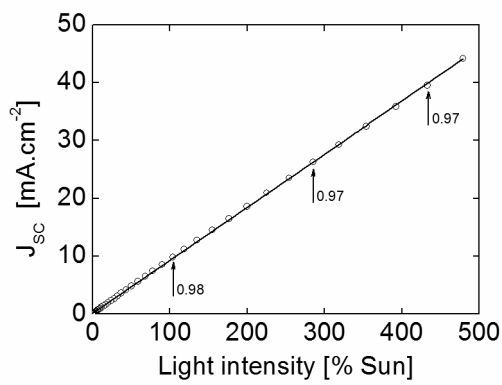


Figure S4: BTT-DPP-90/PC₇₀BM device J_{SC} vs. light intensity. The arrows point out the result of power law fits over different range of illuminations.

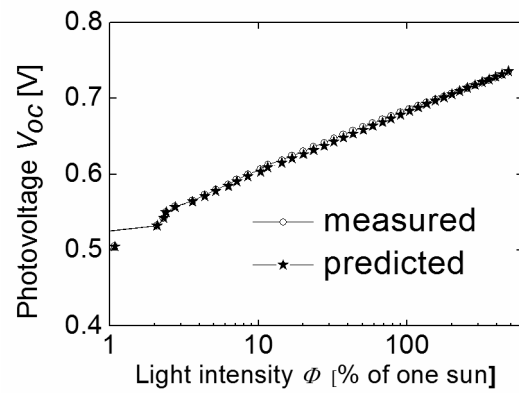


Figure S5: Prediction of the photovoltage based on measurements of charge density at open-circuit and carrier lifetime for the illumination range 1%- 600% of one sun for the BTT-DPP-90/PC₇₀BM device.

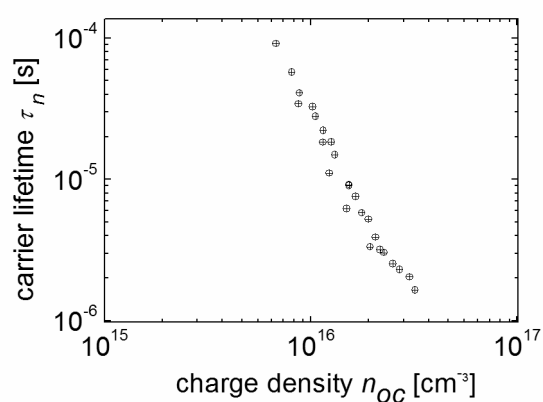


Figure S6: Lifetime of total charge carriers at different charge densities measured using charge extraction at open-circuit and transient photovoltage for the BTT-DPP-90:PC₇₀BM device.

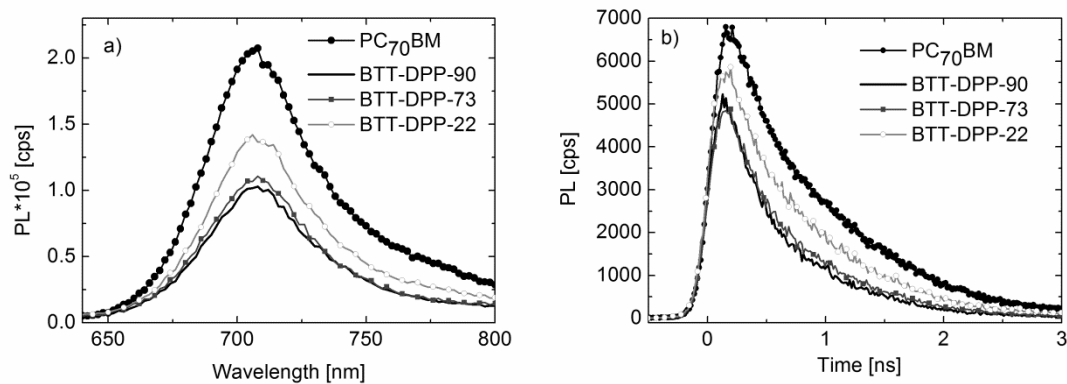


Figure S7: Photoluminescence spectra (a) and decays (b) of BTT-DPP-90:PC₇₀BM, BTT-DPP-₅ 73:PC₇₀BM, BTT-DPP-22:PC₇₀BM blends and neat PC₇₀BM films. Decays were acquired using TCSPC technique with a 200 ps instrument response function. The excitation wavelengths for both experiments were 470 and 467 nm.